Supplementary Material For:

Visible light-driven photocatalytic activity of wide band gap $ATiO_3$ (A=Sr, Zn and Cd) perovskites by lanthanide doping and formation of mesoporous heterostructure with ZnS QDs

Elnaz Zehtab-Lotfi [a], Ali Reza Amani-Ghadim[b,c,*], Behzad Soltani[a]

[a]Department of Chemistry, Faculty of Science, Azarbaijan Shahid Madani University (ASMU), Tabriz 53751-71379, Iran

[b]Applied Chemistry Research laboratory, Department of Chemistry, Faculty of Basic Science, Azarbaijan Shahid Madani University (ASMU), Tabriz 53751-71379, Iran

[c] New Technologies in the Environment Research Center, Azarbaijan Shahid Madani University (ASMU), Tabriz 53751-71379, Iran

Corresponding Author's E-mail addresses:

a.r_amani@yahoo.com; amani.gh@azaruniv.ac.ir

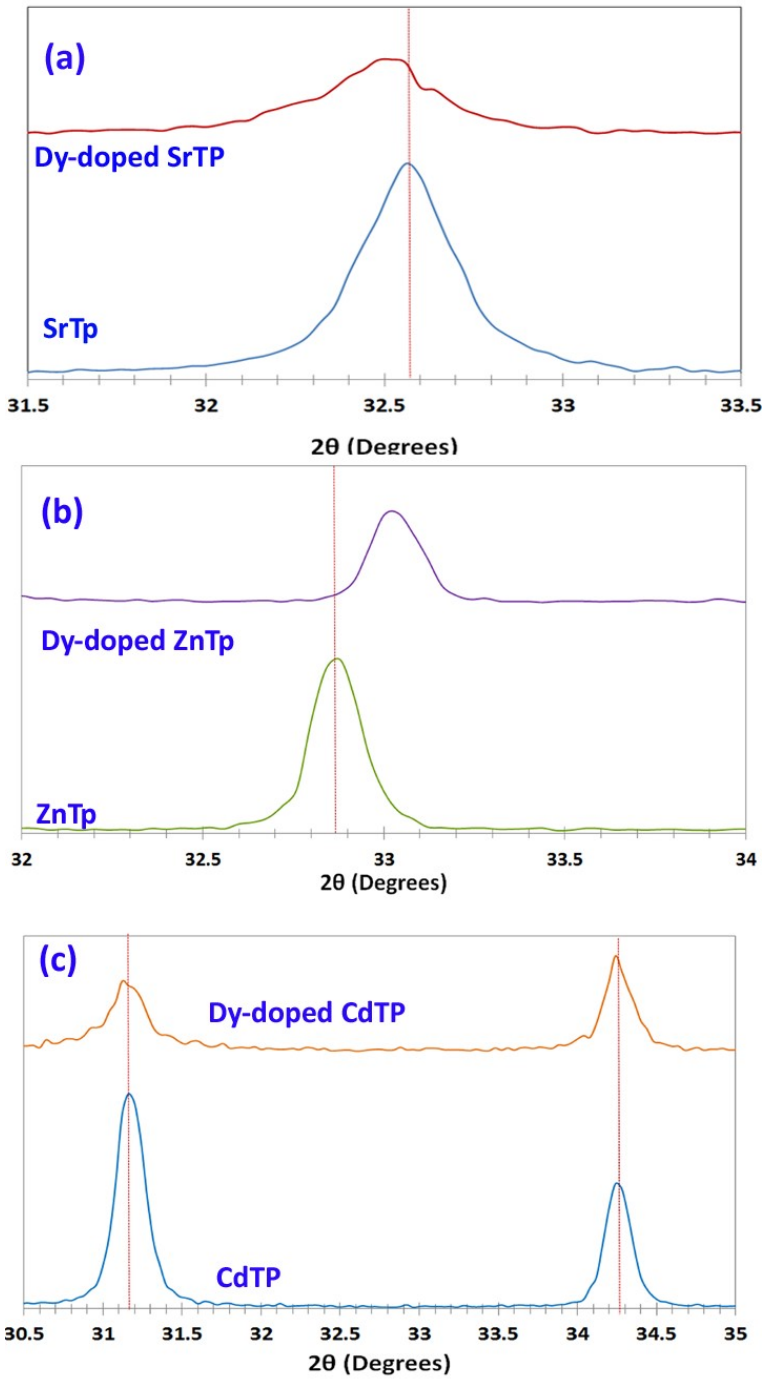

Fig. S1. Enlarged XRD patterns of $ATiO_3$ (A=Sr, Zn and Cd) and Dy-doped $ATiO_3$ samples.

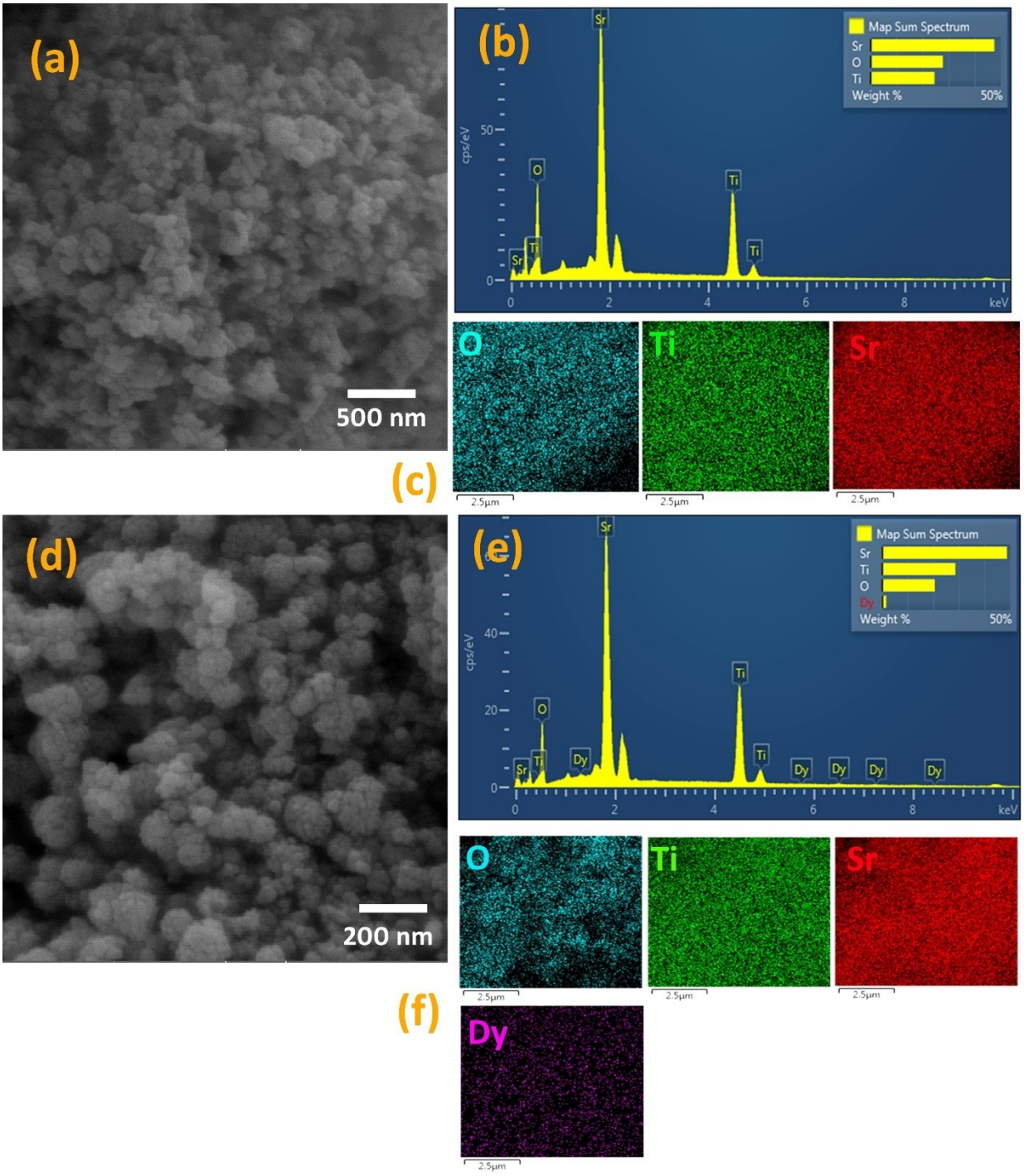

Fig. S2. FESEM images and EDX spectrum accompanied by EDX mapping for SrTP (a-c) and Dy doped-SrTP (d-f).

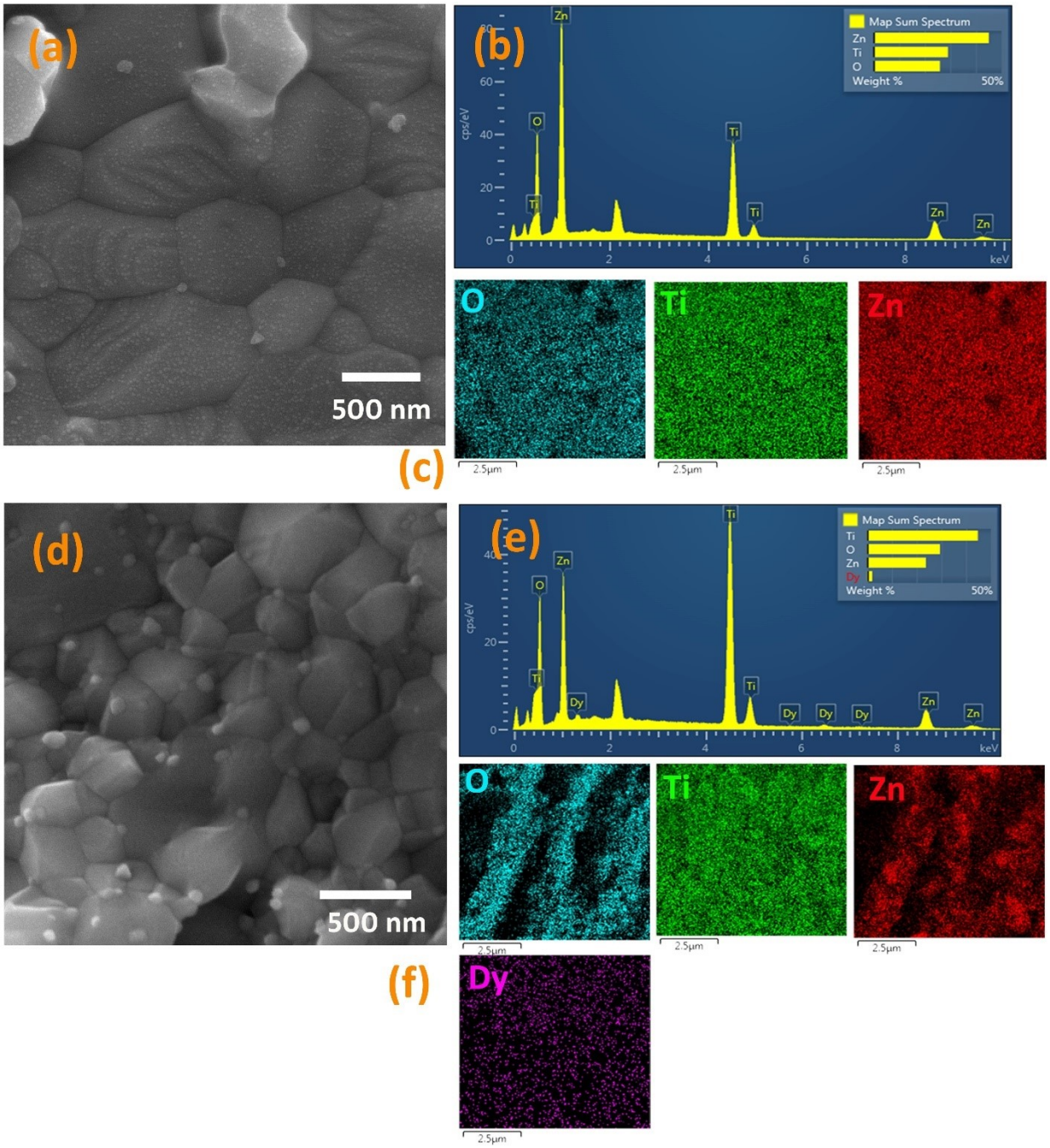

Fig. S3. FESEM images and EDX spectrum accompanied by EDX mapping for ZnTP (a-c) and Dy doped-ZnTP (d-f).

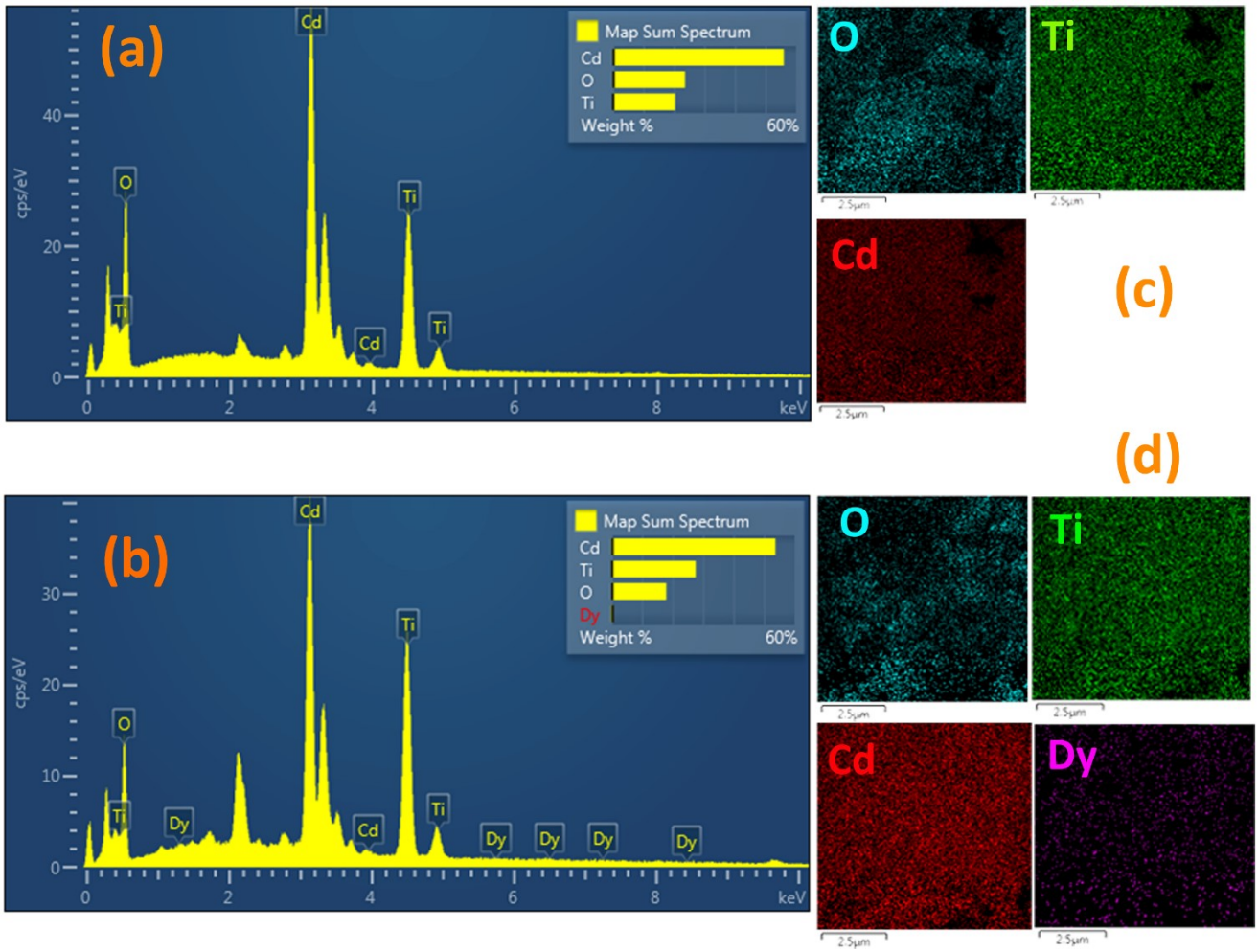

Fig. S4. EDX spectrum accompanied by EDX mapping for CdTP (a, b) and Dy doped-CdTP (c-d).

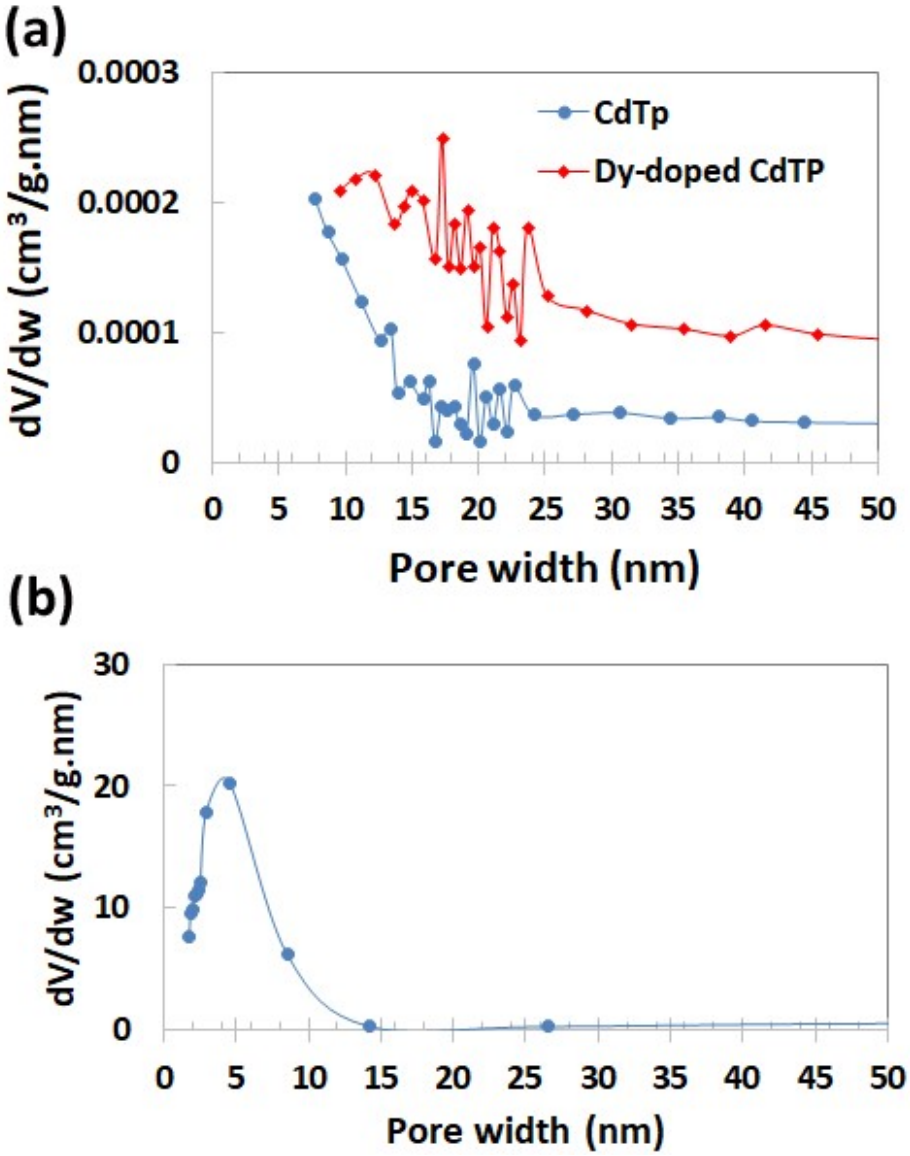

Fig. S5. BJH pore size distribution curves of (a) CdTP and Dy-doped CdTP and (b) Dy-CdTP(0.6)/ZnS QD nanocomposite

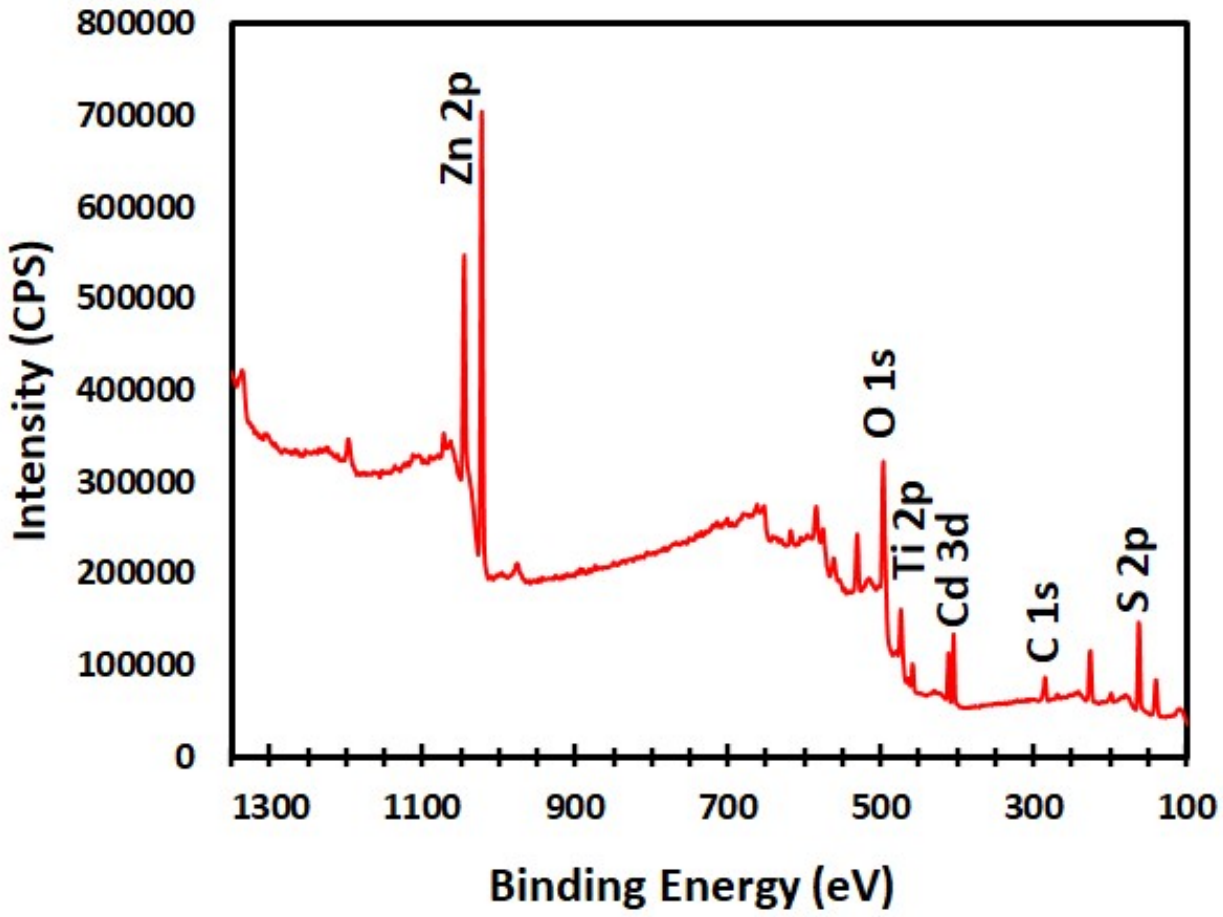

Fig. S6. XPS survey spectra of Dy-CdTP(0.6)/ZnS QD nanocomposite.

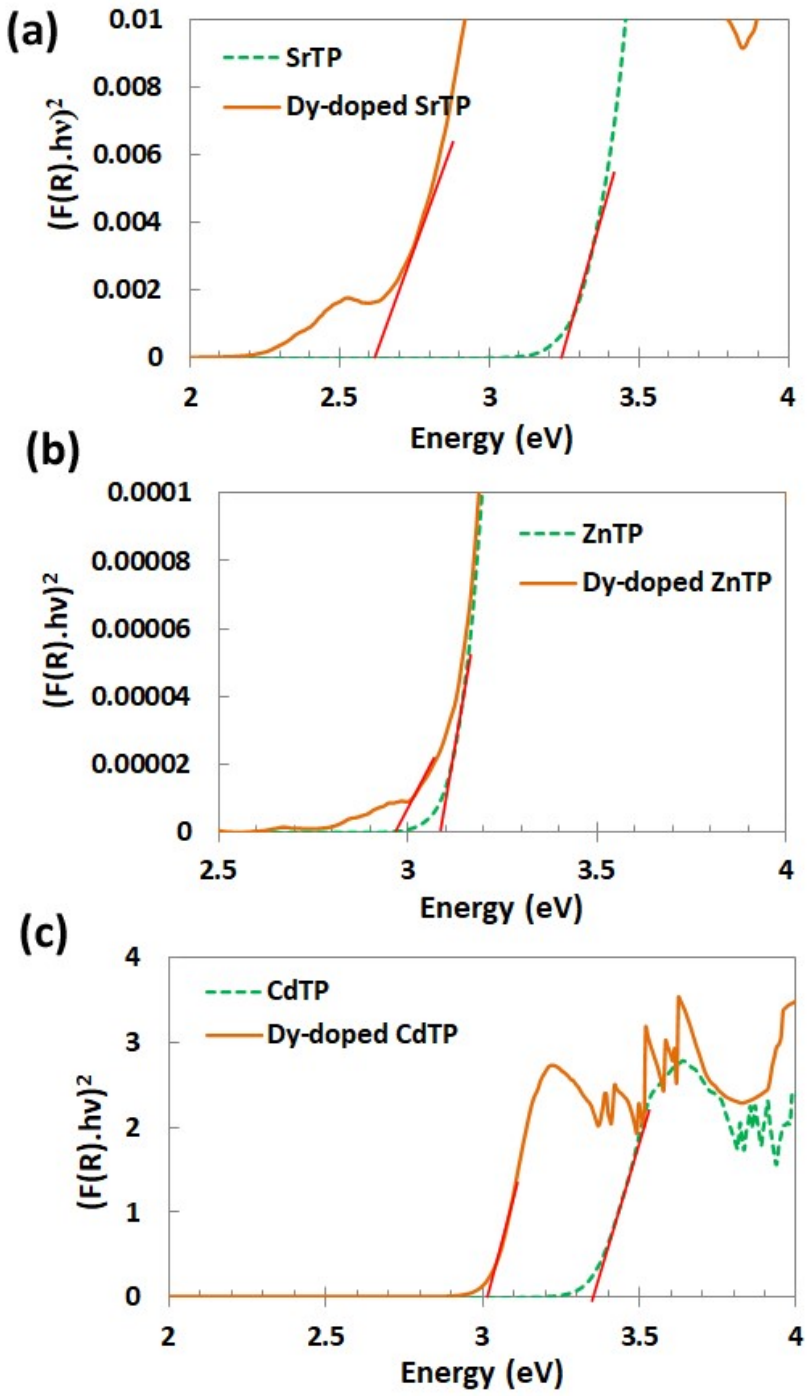

Fig. S7. Kubelka-Munk function vs. the energy of incident light plots of (a) SrTP and Dy-doped SrTP, (b) ZnTP and Dy-doped ZnTP, and (c) CdTP and Dy-doped CdTP.

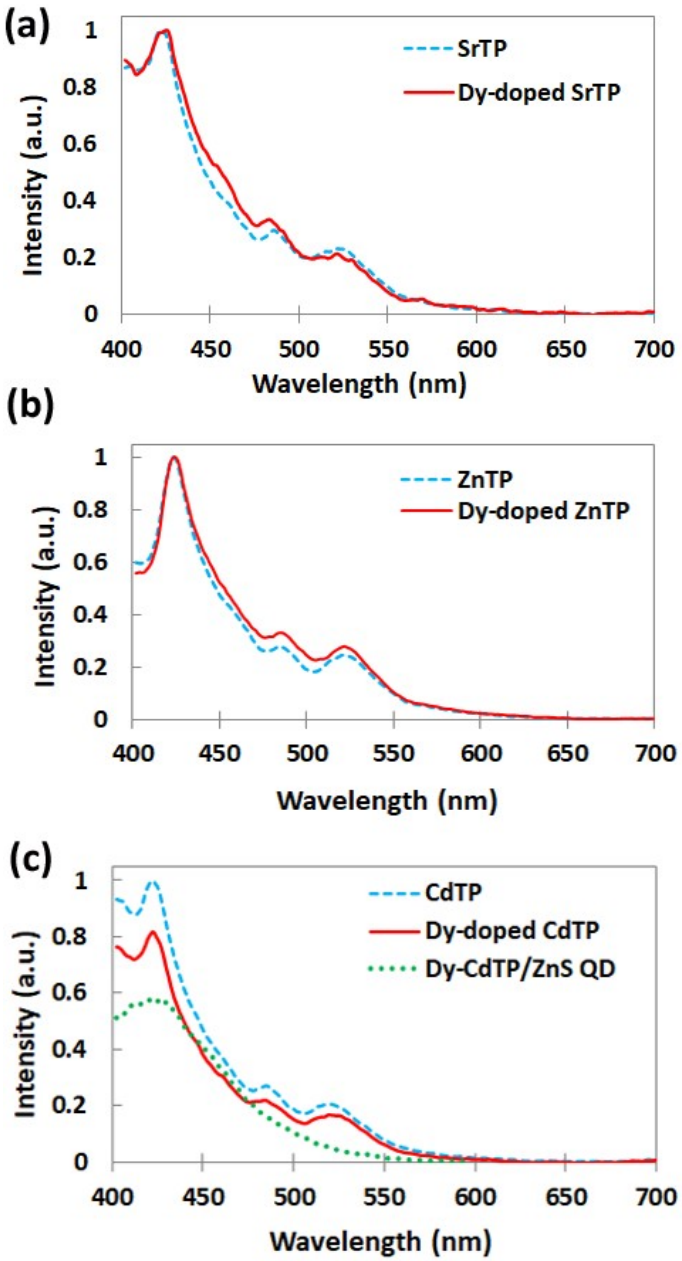

Fig. S8. PL spectra (excited at 380 nm) (a) SrTP and Dy-doped SrTP, (b) ZnTP and Dy-doped ZnTP, and (c) CdTP, Dy-doped CdTP and Dy-CdTP(0.6)/ZnS QD nanocomposite.

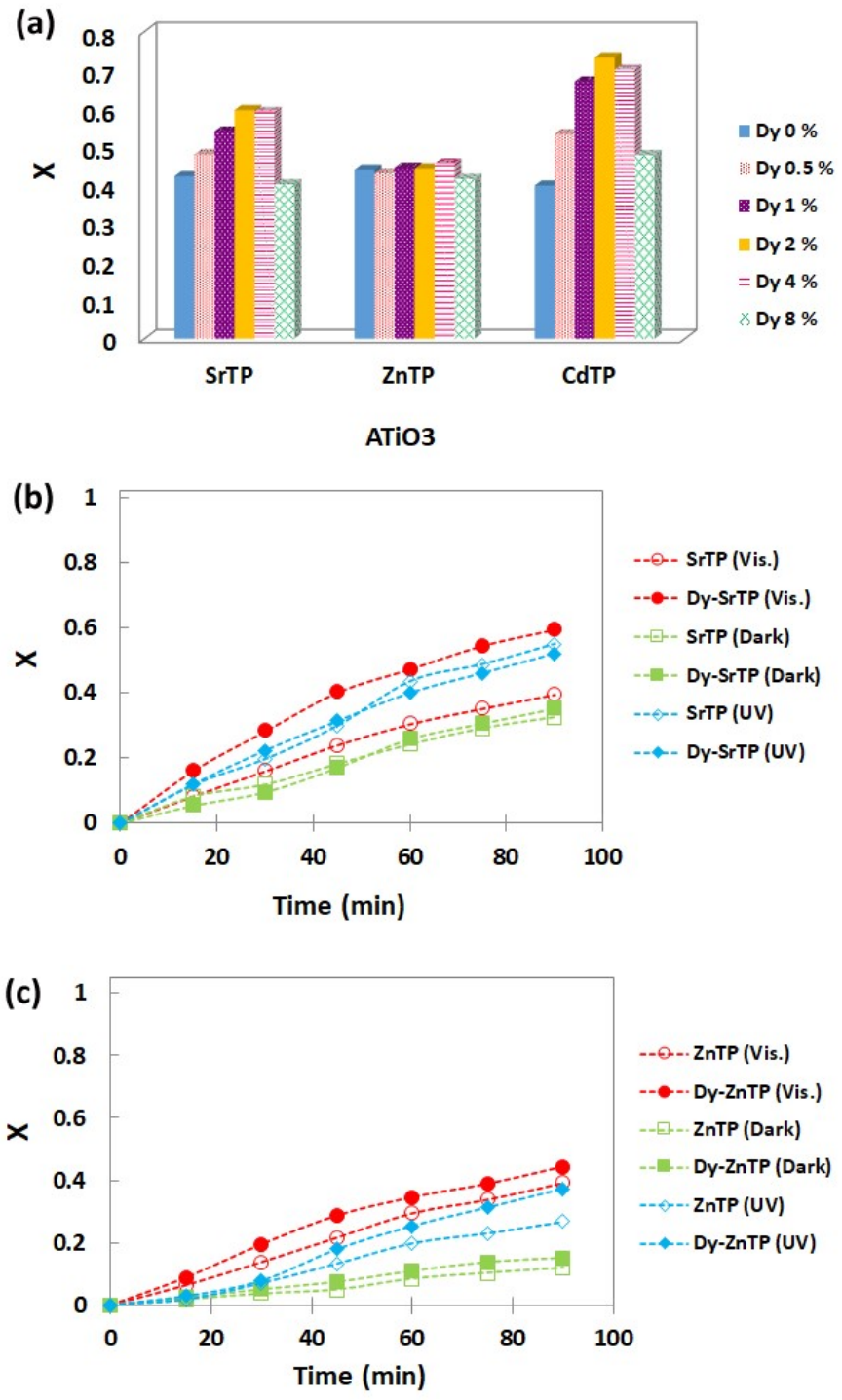

Fig. S9. (a) photocatalytic activity of doped $ATiO_3$ with different doping levels (i.e. 0.5, 1, 2, 4, 8% of Dy cation), (b) photocatalytic performance of SrTP and Dy-doped SrTP, and (c) ZnTP and Dy-doped ZnTP in degradation of MB.

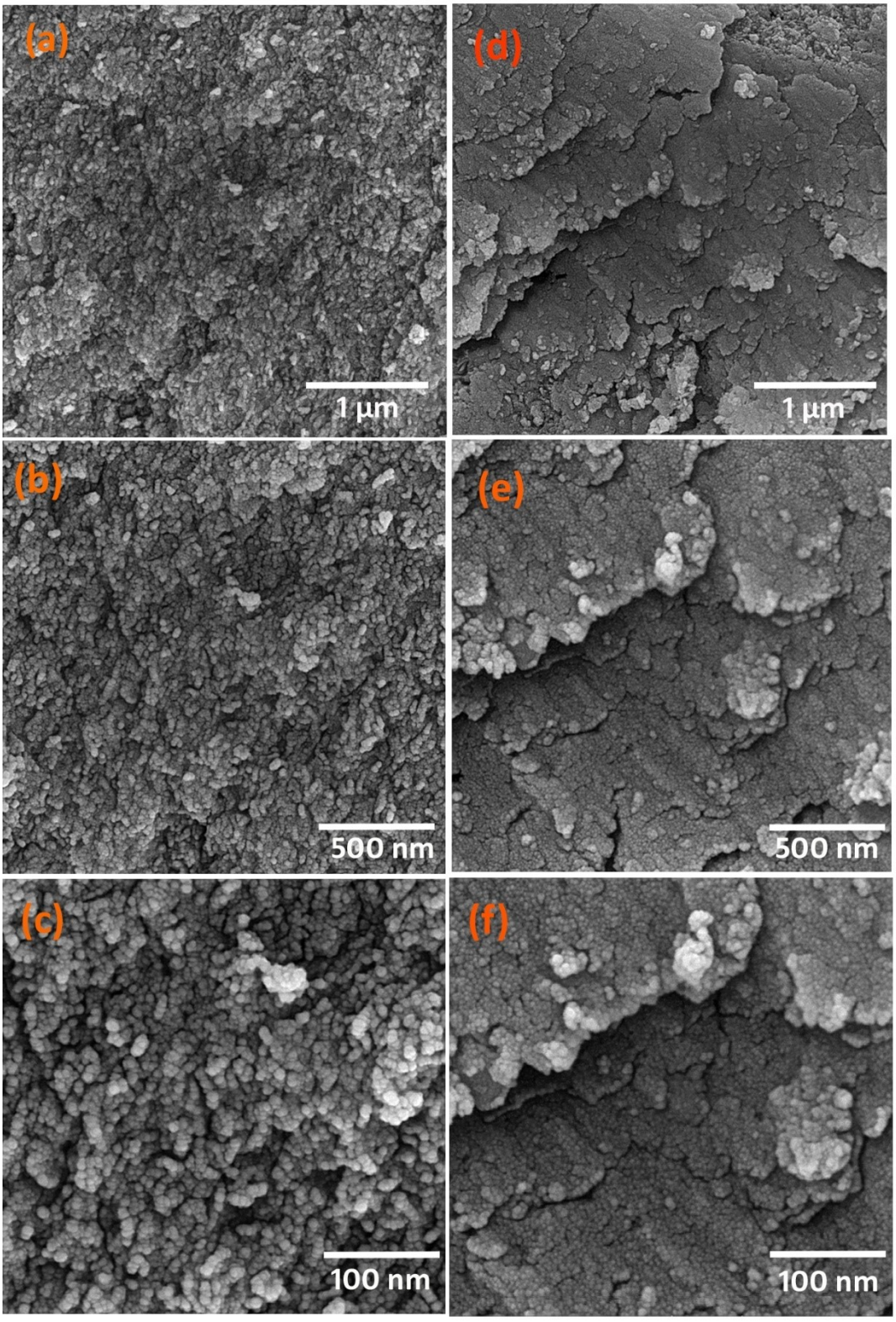

Fig. S10. FESEM images of Dy-CdTP(0.6)/ZnSQDs before (a, b and c) and after (d,e and f) five photocatalytic tests in degradation of MB.

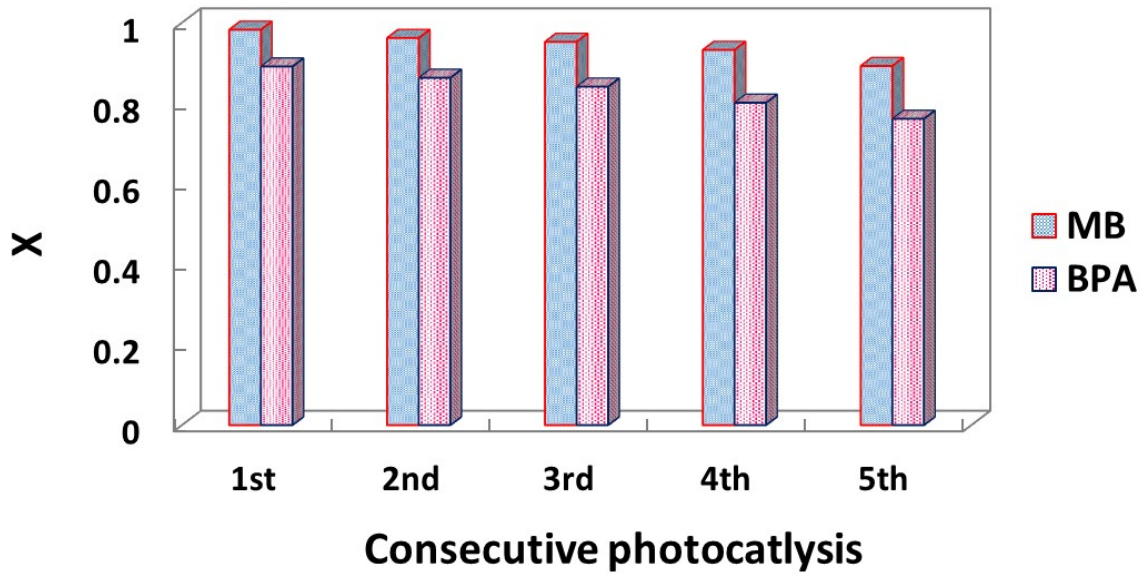

Fig. S11. Sycling photocatalytic stability test of as-prepared Dy-CdTP(0.6)/ZnSQDs photocatalyst.

Table S1. $CdTiO_3$ and ZnS QDs based photocatalysts and their photocatalytic applications.

Photocatalyst	Target	Experimental conditions	Activity	Ref.
$CdTiO_3/CuFe_2O_4$	MB[1], RhB[2], and MO[3]	400 W high-pressure mercury lamp, 25 mg/L of Pollutant and 100 mg/L of Cat., $[H_2O_2]$=0.15 mol/L	≥95 (90 min)	1
CdTiO3/RGO	MB	Ultraviolet-C (λUV= 365 nm), 10 mg/L of Pollutant and 500 mg/L	80 (180 min)	2
CdTiO3@S	CR[4] and CV[5]	Sun light, 10 mg/L of Pollutant and 1000 mg/L of Cat.	89% (60 min) for CV and 91% (60 min) for CR	3
$CdO + CdTiO_3$	MB	LED light, 2.5×10^{-5} mol/L of Pollutant	≥95 (300 min)	4
ZnS QDs/MZnAl-LDH (M=Co or Mn)	AR14[6]	300 W Xenon lamp (λ≥ 420 nm), 50 mg/L of Pollutant and 200 mg/L of Cat.	≥95% (60 min)	5
ZnS QDs-mesoporus TiO_2	MB	Xenon lamp, 10 mg/L of Pollutant and 50 mg/L of Cat.	100% (32 min)	6
$CuInS_2$/ZnS QDs	RhB[7]	500 W high−pressure Hg lamp (λ≥ 420 nm), 10 mg/L of Pollutant and 600 g/L of Cat.	≥95% (120 min)	7
Cu-doped ZnS QDs/TiO_2	Salicylic acidc	Fluorescent lamp (365 nm, I = 1.5 mW/cm^2), 10 mg/L of Pollutant.	90% (150 min)	8
ZnS QDs/RGO	MB	High pressure Hg lamp (365 nm), 10 mg/L of Pollutant and 200 mg/L of Cat.	≥90% (120 min)	9
ZnS QDs-TiO_2 nanofibers	MB	UV lamp (365 nm), 10 mg/L of Pollutant and photocatalyst films (area of 1×1 cm^2.	≥90% (450 min)	10
Gd-doped ZnS QDs/g-C_3N_4	MB and BA[8]	300 W Xenon lamp (λ≥ 420 nm), 20 mg/L of Pollutant and 200 mg/L of Cat.	95% (90 min) for AR14 and 81% (180 min) for BA and	11
Dy-doped $CdTiO_3$/ZnS	MB and BA	300 W Xenon lamp (λ≥ 420 nm), 20 mg/L of Pollutant and 200 mg/L of Cat.	≥95% (60 min) for AR14 and 89% (180 min) for BA and	This Work

[1]Methylene Blue, [2]Rhodamine B, [3]Methyl Orange, [4]Congo Red, [5]Crystal Violet, [6]Acid Red 14, [7]Rhodamin B, [8]Bisphenol A

References:

1. K. Jahanara and S. Farhadi, *RSC Advances*, 2019, **9**, 15615-15628.
2. B. Pant, M. Park and S.-J. Park, *Materials Letters*, 2018, **228**, 365-368.
3. T. Tavakoli-Azar, A. R. Mahjoub, M. S. Sadjadi, N. Farhadyar and M. H. Sadr, *Journal of Inorganic and Organometallic Polymers and Materials*, 2020, **30**, 4858-4875.
4. M. E. de Anda Reyes, G. Torres Delgado, R. Castanedo Pérez, J. Márquez Marín and O. Zelaya Ángel, *Journal of Photochemistry and Photobiology A: Chemistry*, 2012, **228**, 22-27.
5. A. R. Amani-Ghadim, F. Khodam and M. S. Seyed Dorraji, *Journal of Materials Chemistry A*, 2019, **7**, 11408-11422.
6. S. Harish, M. Sabarinathan, A. P. Kristy, J. Archana, M. Navaneethan, H. Ikeda and Y. Hayakawa, *RSC Advances*, 2017, **7**, 26446-26457.
7. W. Zhang and X. Zhong, *Inorganic Chemistry*, 2011, **50**, 4065-4072.
8. H. Labiadh, T. B. Chaabane, L. Balan, N. Becheik, S. Corbel, G. Medjahdi and R. Schneider, *Applied Catalysis B: Environmental*, 2014, **144**, 29-35.
9. M. Wei, Y. Hong, D. Han, L. Yang, H. Liu and L. Su, *physica status solidi (a)*, 2018, **215**, 1800082.
10. S. Chaguetmi, F. Mammeri, S. Nowak, P. Decorse, H. Lecoq, M. Gaceur, J. Ben Naceur, S. Achour, R. Chtourou and S. Ammar, *RSC Advances*, 2013, **3**, 2572-2580.
11. A. R. Amani-Ghadim, S. Arefi-Oskoui, R. Mahmoudi, A. T. Sareshkeh, A. Khataee, F. Khodam and M. S. Seyed Dorraji, *Chemosphere*, 2022, **295**, 133917.